The American Journal of Pathology, Vol. 169, No. 2, August 2006

DOI: 10.2353/ajpath.2006.050876

Tumorigenesis and Neoplastic Progression

Relaxin Enhances the Oncogenic Potential of Human Thyroid Carcinoma Cells

Sabine Hombach-Klonisch,*† Joanna Bialek,‡ Bogusz Trojanowicz,‡ Ekkehard Weber,§ Hans-Jürgen Holzhausen,¶ Josh D. Silvertown,‖ Alastair J. Summerlee,** Henning Dralle,‡ Cuong Hoang-Vu,‡ and Thomas Klonisch*††

From the Departments of Human Anatomy and Cell Science, Obstetrics, Gynecology, and Reproductive Sciences,† and Medical Microbiology,†† University of Manitoba, Winnipeg, Manitoba, Canada; the Division of Stem Cell and Developmental Biology,‖ Ontario Cancer Institute, University Health Network, University of Toronto, Toronto, Ontario, Canada; Biomedical Sciences,** University of Guelph, Guelph, Canada; and the Clinics of General, Visceral, and Vascular Surgery,‡ and the Departments of Physiological Chemistry§ and Pathology,¶ Martin Luther University, Halle/Saale, Germany*

The role of members of the insulin-like superfamily in human thyroid carcinoma is primarily unknown. Here we demonstrate the presence of RLN2 relaxin and relaxin receptor LGR7 in human papillary, follicular, and undifferentiated anaplastic thyroid carcinoma suggesting a specific involvement of relaxin-LGR7 signaling in thyroid carcinoma. Stable transfectants of the *LGR*7-positive human follicular thyroid carcinoma cell lines FTC-133 and FTC-238 that secrete bioactive proRLN2 revealed this hormone to act as a multifunctional endocrine factor in thyroid carcinoma cells. Although RLN2 did not act as a mitogen, it acted as an autocrine/paracrine factor and significantly increased anchorage-independent growth and thyroid carcinoma cell motility and invasiveness through elastin matrices. Suppression of *LGR*7 expression by *LGR*7-siRNA abolished the RLN2-mediated accelerated tumor cell motility. The increased elastinolytic activity correlated with enhanced production and secretion of the lysosomal proteinases cathepsin-D (cath-D) and cath-L forms hereby identified as new RLN2 target molecules in human neoplastic thyrocytes. We found the intracellular distribution of procath-L specifically altered in RLN2 transfectants, providing first evidence for selective actions of relaxin on the powerful elastinolytic cath-L production, storage, and secretion in thyroid carcinoma cells. Thus, relaxin enhances the oncogenic potential and acts as novel endocrine modulator of invasiveness in human thyroid carcinoma cells. ***(Am J Pathol 2006, 169:617–632; DOI: 10.2353/ajpath.2006.050876)***

In recent years, the multifunctional peptide hormone relaxin has been identified as an important endocrine player in the reproductive tract, cardiovascular/neural systems, and oncology.[1,2] The thyroid was once considered to be a relaxin target tissue with relaxin reported to increase thyroid weight, radioactive iodine uptake, and protein-bound iodination in rats.[3,4] Likely because of the crude relaxin preparations used at the time, these results could not be confirmed.[5] No further investigations were reported thereafter using highly purified relaxin preparations to validate a potential role of relaxin in thyroid tissues and thyroid cell lines. Some 40 years later, the discovery of the G-protein-coupled relaxin-like receptors LGR7 and LGR8 revealed the presence of transcripts for both *LGR7* (relaxin receptor) and *LGR8* (INSL3/relaxin receptor) in the thyroid gland.[6–8]

Relaxin and the relaxin-like INSL3 have been shown to activate cAMP-dependent signaling pathways by binding to either LGR7 or LGR8.[8–12] We recently demonstrated the expression and regulation of INSL3 and *LGR8* transcripts in human thyroid carcinoma cell lines, identifying hyper- and neoplastic human thyrocytes as a new source and target of the actions of INSL3 and a novel INSL3 splice variant.[8,13]

Although still primarily undefined, relaxin appears to have oncogenic potential in various organs and tissues, including the human thyroid.[14–17] Relaxin affects proliferation and differentiation of MCF-7 human carcinoma cells in a concentration-dependent manner[18] and can modify the extracellular matrix by affecting the expres-

Supported by the Deutsche Forschungsgemeinschaft (grants KL1249/5-1 and KL1249/5-2) and the Wilhelm Roux Program, Medical Faculty, Martin Luther University Halle-Wittenberg.

S.H.-K. and J.B. contributed equally to this study.

Accepted for publication April 13, 2006.

Address reprint requests to Dr. Thomas Klonisch, Dept. of Human Anatomy and Cell Science, Faculty of Medicine, University of Manitoba, 130 Basic Medical Sciences, 730 William Ave., Winnipeg, MB, R3E 0W3, Canada. E-mail: klonisch@cc.umanitoba.ca.

sion of matrix metalloproteinases (MMPs), which potentially contribute to relaxin's role as a migration-promoting peptide in mammary carcinoma cells of different species,[15] including humans.[19]

In the present study, we have for the first time revealed novel roles for RLN2 in human thyroid carcinoma cells. We identified neoplastic thyroid tissues as a source of RLN2 and LGR7, implicating an active RLN2-LGR7 signaling system in human thyroid carcinoma. Enhanced metabolic activity, anchorage-independent growth, and increased migratory and elastinolytic activity were among the phenotypes observed with stable transfectants of the human follicular thyroid carcinoma cell lines, FTC-133 and FTC-238, which overexpress and secrete bioactive proRLN2. Finally, relaxin up-regulated the production and secretion of cath-L and cath-D, identifying this insulin-like peptide hormone as a novel modulator of the oncogenic potential of human thyroid carcinoma cells.

Materials and Methods

Thyroid Tissues

A total of 59 thyroid tissues, including 10 goiter tissues, 9 Graves' disease tissues, and 14 papillary thyroid carcinomas (PTCs), 12 follicular thyroid carcinomas (FTCs), and 14 undifferentiated thyroid carcinomas (UTCs), were collected from patients at the Department of Surgery, University of Halle, by surgical resection for clinical indications (Table 1). This study was approved by the ethical committee of the Martin Luther University, Faculty of Medicine, and all patients gave written consent. Tissues were fixed in formalin and embedded in paraffin and cryopreserved in liquid nitrogen. The human thyroid papillary carcinoma cell line BC-PAP; the follicular carcinoma cell lines FTC-133, FTC-236, FTC-238; and the anaplastic carcinoma cell lines Hth74, C643, UTC-8305, and UTC-8505 were propagated in Dulbecco's minimal essential medium (DMEM)/Ham's F12 (Biochrom, Berlin, Germany) supplemented with 10% fetal calf serum (FCS) in a 5% CO_2 atmosphere at 37°C. Medium was changed every second day, and cells were routinely passaged every 3 to 5 days.

Total RNA Extraction and Reverse Transcriptase-Polymerase Chain Reaction (RT-PCR)

Total RNA was extracted from the human thyroid cell lines and tissues for RT-PCR analysis using the Trizol reagent (Life Technologies, Karlsruhe, Germany) and RNeasy extraction kit (Qiagen, Hilden, Germany), respectively, according to the manufacturers' protocols. The amount of isolated total RNA was determined by spectrophotometry at 260 and 280 nm.[20] One μg of total RNA was used for first-strand cDNA synthesis using the Superscript reverse transcriptase kit and 500 ng/ml of oligo d(T) primer (both Life Technologies). Total RNA was also isolated from the human follicular thyroid carcinoma cell lines. For the amplification of *RLN2* prorelaxin and the partial coding sequence of human *LGR7* relaxin receptor, specific intron-spanning oligonucleotide primers (Table 2) were used to preclude any genomic DNA amplification. Before semiquantitative RT-PCR analysis with the Bio 1D software (LTF, Wasserburg, Germany), cDNA samples were adjusted to equal 18S RNA input. RT-PCR reactions were performed in a 25-μl solution containing 2 μl of cDNA, 2.5 μl of 10× Advantage2 polymerase mix buffer, 10 nmol/L of dNTP, 20 pmol of each primer (Table 2), and 2 U *Taq*DNA-polymerase (Life Technologies). PCR cycles consisted of an initial denaturation for 5 minutes at 95°C, followed by 35 cycles of denaturation at 95°C for 45 seconds, annealing for 45 seconds (for temperatures see Table 2), elongation for 1.5 minutes at 72°C, and a final extension cycle for 10 minutes at 72°C. PCR products were separated on a 1% low-melting point agarose gel. For sequence analysis, amplicons were purified by Magic column extraction, cloned into the

Table 1. List of Thyroid Papillary (PTC), Follicular (FTC), and Dedifferentiated Anaplastic Thyroid Carcinoma Tissues (UTC) Used in This Study

Tissue	Gender	Age	PTNM
PTC (n = 14)	M	25	T4aN1bM1
	F	**51**	**T4N1aM0**
	F	**56**	**T4N1bM1**
	F	14	T4N0M0
	F	14	T4N1M0
	M	65	T3N1Mx
	F	71	T3N1M1
	M	11	T3N1Mx
	M	36	T2N1Mx
	M	63	T2aN0M0
	F	27	T2N1aMx
	F	59	T1N0M0
	F	39	T1N0M0
	F	55	T1aN0M0
FTC (n = 12)	**F**	**53**	**T4N0M0**
	F	60	T4NxM1
	F	62	T4N1bM1
	F	34	T4N0M0
	F	**60**	**T4N0M0**
	M	60	T4NxM2
	F	51	T3N1bM0
	M	67	T3bN1bM1
	M	43	T3N0M0
	M	63	T3N0M0
	F	46	T3NxM0
	F	54	T2NxMx
UTC (n = 14)	F	79	T4N2Mx
	F	72	T4N2Mx
	F	76	T4N1Mx
	F	**58**	**T4N1Mx**
	F	70	T4N1aMx
	M	67	T4N1Mx
	F	87	T4N0M1
	F	53	T4N0M1
	F	75	T4N0M1
	F	68	T4N0M1
	F	42	T4N0M1
	M	66	T4N0M0
	F	69	T3NxMx
	M	52	T3N0M0

M, male; F, female. Those thyroid carcinoma tissues devoid of RLN2 mRNA and immunoreactive protein are indicated in bold.

Table 2. Oligonucleotide Primers Used at Melting Temperatures (T_M) Used to Determine the Expression of *RLN2*, Human *LGR7* Relaxin Receptor, and *18S* Transcripts in Human Thyroid Carcinoma Cell Lines

Primer	Primer sequence	bp	T_M (°C)
Forward RLN2	5′-CGGACTCATGGGATGGAGGAAG-3′	222	61
Reverse RLN2	5′-GCTCCTGTGGCAAATTAGCAAC-3′		
Forward huLGR7	5′-CCCAATTCTCTATACTCTGACCACAAG-3′	243	65
Reverse huLGR7	5′-TCATGAATAGGAATTGAGTGTCGTTGATT-3′		
Forward 18S	5′-GTTGTTGGAGCGATTTGTCTGG-3′	344	61
Reverse 18S	5′-AGGGCAGGGACTTAATCAACGC-3′		

pGEM-T vector (both Promega, Heidelberg, Germany), and sequenced in both directions using the PRISM dye Deoxy Terminator cycle sequencing kit (Perkin-Elmer, Foster City, CA) and T7 or SP6 sequencing primers.

Generating Stable Transfectants Overexpressing proRLN2

For stable transfection of FTC133 and FTC-238 with the pCMV-preproRLN2-IRES-EGFP[15] or the pCMV-IRES-EGFP vector (Clontech, Heidelberg, Germany) we used the Lipofectamine 2000 kit according to the manufacturer's protocol (Life Technologies). Both plasmids had been purified using the DNA Midi isolation kit (Qiagen). Stably transfected clones with the pCMV-preproRLN2-IRES-EGFP (FTC-133, 12 clones; FTC-238, 1 clone) and pCMV-IRES-EGFP vector (FTC-133, 9 clones; FTC-238, 3 clones), respectively, were selected, maintained in medium containing with 800 μg/ml geneticin (Life Technologies), and displayed bright EGFP production in fluorescence microscopy (Zeiss, Jena, Germany). Of those, three FTC-133- and one FTC-238-pCMV-preproRLN2-IRES-EGFP transfectants expressing relaxin transcripts (FTC-133-RLN2 and FTC-238-RLN2) and two clones each of FTC-133 and FTC-238 containing the pCMV-IRES-EGFP vector (FTC-133-EGFP and FTC-238-EGFP) were used in this study. In all assays performed, similar responses were obtained for all RLN2 transfectants when compared with EGFP controls. A medium change was performed every 2 to 3 days and transfectants were passaged every 3 to 5 days using accutase (PAA Laboratories GmbH, Linz, Austria). Before experimentation, cells were seeded at the desired cell densities either in 25-cm^2 flasks or in 6-, 24-, or 96-well plates on the day of experimentation (Techno Plastic Products AG, Trasadingen, Switzerland).

Small Interfering (si) RNA

The day before transfection FTC-133 cells were seeded at 10^4 cells/well on a six-well plate. Cells were washed three times in phosphate-buffered saline (PBS) before transfection with nonsilencing- or *LGR7*-siRNA (Qiagen). The nonsilencing siRNA (siNC) conjugated to Alexa Fluor 555 with no sequence similarity to human gene sequences was used as a control (1027099: 5′-AATTCTCCGAACGTGTCACGT-3′). The following *LGR7*-siRNA target sequences were used: a single *LGR7*-siRNA at a final concentration of 300 nmol/L 5′-CTGCAGTTACCTGCTTTGGAA-3′ (exon 15) and a combination of two human LGR7-siRNAs at a concentration of 50 nmol/L each 5′-GCTCCAGACCTTGGCAAAGAC-3′ (exon 4) and 5′-TACTAGATAGGAATTGAGTCTC GTTGATT-3′ (exon 20) were found to be optimal. The Lipofectamine 2000 kit (Life Technologies) was used for transfecting the siRNA constructs. After 24 hours the transfection medium was replaced with normal medium. The level of *LGR7* mRNA suppression was highest at 72 hours after transfection. Total RNA was isolated and the level of *LGR7* mRNA was determined by semiquantitative RT-PCR as described above. All siRNA experiments for RT-PCR, cAMP, and motility assays were performed in triplicates of three independent samples (see below).

Enzyme-Linked Immunosorbent Assay (ELISA)- and Fluorometric-Based Assays

Relaxin ELISA

Transfectants were seeded at 5×10^4 cells/well of a six-well plate and cultured in 1 ml of culture medium for 24 hours in a humidified CO_2 incubator. Secreted relaxin in conditioned medium (200 μl) was determined by ELISA according to the manufacturer's instructions (Immunodiagnostic, Bensheim, Germany). The color reaction was determined at 450 nm with an ELISA reader (SLT Labinstruments GmbH, Crailsheim, Germany).

cAMP Assay

Intracellular cAMP levels were determined in FTC-133-RLN2, clone 10, at 1×10^4 cells/well cultured for 24 hours in 96-well plates. Cells were preincubated with 3-isobutyl-1-methyl-xanthine (IBMX; Sigma, Munich, Germany) at 1 mmol/L for 2 hours at 37°C in a water-saturated CO_2-incubator. The medium was replaced with 1 ml of 1) fresh medium containing 10 μmol/L forskolin as a positive control (Merck Biosciences, Bad Soden, Germany); 2) supernatants from one FTC-133-EGFP clone as negative control; 3) supernatants from FTC-133-RLN2 clones 4, 10, 11. Supernatants (200 μl) had been collected from six-well plate cultures of FTC-133-EGFP and FTC-133-RLN2, clones (8×10^4 cells/well) after 24 hours of culture and centrifuged at $3000 \times g$ for 30 minutes to remove remaining cells. FTC-133-RLN2 clone 10 cells (1×10^4 cells/well) were incubated with these media/supernatants, all containing 1 mmol/L IBMX, for 1 hour at 37°C in a water-saturated CO_2 incubator. Cells were harvested, washed,

and lysed with cAMP extraction buffer and cAMP levels were detected with the colorimetric cAMP Biotrak enzyme immunoassay (Amersham, Freiburg, Germany). The reaction was stopped in 1 mol/L H_2SO_4 and the product was measured at 450 nm in a microplate reader (SLT).

BrdU Assay

A colorimetric BrdU cell proliferation ELISA (Roche Diagnostics, Mannheim, Germany) was used according to the manufacturer's instructions. Briefly, on the day of assay, 20 μl of BrdU labeling solution were added to each well of a 96-well plate, except for negative controls that received no BrdU. Cells were incubated for 2 hours at 37°C in a water-saturated CO_2 incubator. The assay was performed with 0.25, 0.5, and 1×10^4 stable transfectants/100 μl medium. Thereafter, plates were drained, air-dried for 20 minutes, and blocked with 200 μl/well of ELISA blocking reagent (Roche) for 30 minutes at room temperature. After decanting, 100 μl of BrdU antiserum was added to each well and dishes were incubated for 30 minutes at room temperature. Plates were drained, washed, and incubated with 100 μl/well of substrate solution for 10 minutes at room temperature. Finally, 25 μl of 1 mol/L H_2SO_4 were added to each well, incubated for 1 minute on a shaker at 300 rpm, and absorbance was measured within 5 minutes at 370 nm in an ELISA reader (SLT).

Cell Cytotoxicity (MTT) Assay

The cytotoxicity Easy-for-You assay kit (Biomedica, Wien, Austria) was performed in 96-well plates according to the manufacturer's instructions. Stable transfectants were plated in 200 μl of medium at 0.25, 0.5, and 1×10^4 cells/well and grown overnight in a CO_2 incubator. On addition of chromophorous substrate (20 μl) for 2 hours, $NADH_2$-dependent colored formazan salt formation was monitored hourly for 4 hours at 450 nm using an ELISA reader (SLT).

Luminometric ATP Assay

Stable transfectants plated in 96-well plates at a density of 0.25, 0.5, and 1×10^4 cells/well in 100 μl of medium were allowed to grow overnight at 37°C in a CO_2 incubator. Wells devoid of cells served as blank. Substrate (100 μl) was added to each well (CellTiter-Glo Luminescent; Promega) and incubated on a shaker and on the benchtop for 2 minutes and 10 minutes at room temperature, respectively. Luminescence was measured with a Sirius luminometer (Berthold Detection Systems GmbH, Pforzheim, Germany).

Soft Agar Assay

Two-layered soft agar assays were performed in six-well plates. The bottom layer of agar (1.5 ml per well) consisted of 5 ml of 3% agar (Roth, Karlsruhe, Germany) in sterile water, 3 ml of FCS (Biochrom), 45 μl of geneticin (50 mg/ml, Life Technologies), 300 μl of a 1:1000 dilution of amphotericin B (stock, 250 μg/ml), and 900 μl of a 1:1000 dilution of gentamicin (stock, 10 mg/ml; all from Sigma) added to 30 ml with Ham's F12 medium. Once solidified at room temperature for 10 minutes, 20,000, 50,000, or 100,000 cells of FTC-133-RLN2 and FTC-133-EGFP were mixed into 1 ml of upper agar layer prepared from a stock consisting of 1.6 ml of 3% agar, 10% FCS, 22.5 μl of geneticin (50 mg/ml), 150 μl (1:1000 dilution) of amphotericin B (250 μg/ml), 450 μl (1:1000 dilution) of gentamicin (10 mg/ml) in 15 ml of culture medium. This cell suspension was carefully layered on top of the bottom layer and once this top agar layer had solidified 1 ml of the culture medium was carefully added and changed once a week. After 4 to 6 weeks, cell colonies in the agar were colored overnight at 37°C in a 5% CO_2 atmosphere with 200 μl of iodo-tetrazolium chloride *in vivo* stain (Sigma). Colored cell colonies were examined by bright-field microscopy (Zeiss).

Motility and Migration Assays

Cellular motility and migration were evaluated in 24-well Transwell chambers (Costar, Bodenheim, Germany). The upper and lower culture compartments were separated by polycarbonate filters with 8-μm pore size. For migration assays, the upper site of the filters (upper chamber) was coated with 50 μg/ml of human elastin (Sigma) before seeding cells. To investigate the effect of recombinant human RLN2 (generously provided by Dr. Laura Parry, University of Melbourne, Melbourne, Australia) on the motility of untransfected thyroid carcinoma cells, FTC-133 or FTC-238 were plated at 1×10^4 cells/well in Ham's F12 medium with or without 10% FCS and incubated for 24 hours in a 5% CO_2 atmosphere at 37°C in the absence or presence of human RLN2 at 100 ng/ml or 500 ng/ml added to the wells (lower chamber). To investigate a similar autocrine/paracrine effect of relaxin secreted by the transfectants, RLN2 and EGFP clones were seeded onto the filter at 1×10^4 cells/well and placed in the well harboring 5×10^4 of either RLN2 or EGFP transfectants (lower chamber). Control experiments were performed to determine the specificity of RLN2-mediated signaling on the motility of FTC-133 and FTC-238 tumor cells seeded on the filter: 1) recombinant RLN2 (500 ng/ml) was heat-inactivated for 10 minutes at 90°C before incubation with the cells; 2) supernatant collected from FTC-133-RLN2, clone 10, grown to confluency in a six-well was diluted 1:1, 1:2, and 1:4 with normal culture medium (v/v) before incubation with FTC-133 on the filter; 3) FTC-133 and FTC-238 were transfected with specific *LGR7* siRNA constructs and motility was determined in the presence or absence of recombinant RLN2 at 100 or 500 ng/ml). After a 16-hour incubation period, cells remaining on top of the filter were wiped off with cotton swabs and those transfectants that had traversed the membrane pores to the lower surface of the membrane were washed with chilled PBS, incubated for 5 minutes in 1:1 PBS/methanol (Merck, Darmstadt, Ger-

many) and 15 minutes in methanol before staining with 0.1% toluidine blue (Merck) in 2.5% sodium carbonate (Roth). Migrated cells were counted by light microscopy (Zeiss) in four separate high-power fields per filter.

Immunohistochemistry and Evaluation

Human paraffin-embedded serial 3-μm thyroid tissue sections (Table 2) were dewaxed and rehydrated in PBS plus 0.1% Tween 20 (PBST). Sections were treated with proteinase K (30 μg/ml; both Sigma) for 30 minutes at 37°C and 3% H_2O_2 in methanol for 25 minutes at room temperature to inactivate endogenous peroxidase activity. Sections were washed in PBST and nonspecific binding sites were blocked with 10% goat serum in PBST (blocking buffer) for 1 hour at room temperature. Detection of immunoreactive RLN2 in the human thyroid tissue sections was performed with two previously characterized rabbit polyclonal antibodies against RLN2. One polyclonal antiserum against RLN2 was from Immunodiagnostik (Bensheim, Germany)[21] and was diluted 1:300 in blocking buffer overnight at 4°C. Serial sections were also immunostained with the R6 rabbit anti-porcine relaxin antiserum (generously provided by Prof. Bernhard Steinetz, Nelson Institute of Environmental Medicine, New York University Medical Center, Tuxedo, NY) at a dilution of 1:800 in blocking buffer at 4°C overnight. Nonimmune rabbit serum (1:300) served as control. As a secondary antibody, horseradish peroxidase-conjugated goat anti-rabbit was used at a dilution of 1:500 for 1 hour at room temperature. After washing in PBST, detection was performed with filtered diaminobenzidine solution for 10 minutes and immunostained sections were counterstained with hematoxylin. Immunoreactive relaxin receptor LGR7 in human thyroid tissues was detected with a previously characterized rabbit polyclonal antiserum against human LGR7 (generously provided by Prof. Aaron Hsueh, Dept. of Obstetrics and Gynecology, Stanford University, Stanford, CA) used at 1:800 in blocking buffer.[8] All immunostained tissue sections (two sections per patient) were evaluated by two independent reviewers blinded to the histological diagnosis. Planimetric measurement of immunostained tissues was performed semiquantitatively using the Axioplan light microscope and the Zeiss KS300 software (Zeiss). The percentage of immunostained tissue areas per total section area (100%) was classified into four groups: 0 to 10% negative; 10 to 40% low; 40 to 80% moderate; ≥80% high.

Immunofluorescence and Confocal Laser-Scanning Microscopy

For immunofluorescent detection of cathepsin-D (cath-D), cathepsin-L (cath-L), mannose-6-phosphate receptors (M-6-PR), and the lysosomal marker CD63, transfectants were plated on sterile glass slides at 2×10^4 cells/ml and incubated in a humidified atmosphere at 5% CO_2 for 2 to 3 days before fixation of cells with 4% formaldehyde. Sections were incubated overnight at 4°C with previously characterized primary rabbit polyclonal antiserum to human cath-D[22] diluted at 1:500 and mouse monoclonal antibodies (mAbs) specific for human procath-L (2D4) and all three cath-L forms (procath-L, single-chain, and heavy chain of cath-L; 33/1)[23,24] at 1:100 each, respectively, in blocking solution (2% bovine serum albumin, 0.05% saponin in PBS; Sigma). Cells were washed with PBST and incubated with 10% goat or donkey antiserum for 30 minutes before a 1-hour incubation with the secondary rhodamine-conjugated goat anti-rabbit antiserum (1:400; Dianova, Hamburg, Germany) or rhodamine-conjugated donkey anti-mouse antiserum (1:100; Jackson ImmunoResearch, West Grove, PA), respectively. Immunofluorescent localization of mannose-6-phosphate receptors (M6PR type I+II; Abcam, Cambridge, UK) and lysosomal marker CD63 (Sigma) was performed with mAbs diluted at 1:200 and 1:1000 in blocking buffer (for M6PR containing 0.05% saponin; Sigma), respectively. After blocking nonspecific binding sites with 10% donkey serum, the secondary rhodamine-conjugated donkey anti-mouse antiserum (1:100; Jackson ImmunoResearch) was used for visualization. In all cases, nuclear Hoechst stain (1:100; Sigma) was used, and labeled cells were embedded in Fluoroguard antifade reagent (Bio-Rad, Munich, Germany) before fluorescence microscopy or confocal laser-scanning microscopy (KLSM-410; both Zeiss).

Western Blot Analysis

For the detection of relaxin, cellular proteins of stable RLN2 and EGFP transfectants as well as untransfected FTC-133 and FTC-238 cells were extracted in RIPA buffer [1% Nonidet P-40, 0.1% sodium dodecyl sulfate (SDS) in PBS] with the addition of protease inhibitor cocktail (all from Sigma). Protein concentrations were determined by Bradford assay (Bio-Rad). Extracted proteins (40 μg) were separated under nonreducing conditions on a 15% SDS gel and blotted at 330 mA for 35 minutes onto Hybond-ECL nitrocellulose membranes (Amersham, Freiburg, Germany). Nonspecific binding sites were blocked for 1.5 hours in blocking buffer [1% milk, 5% bovine serum albumin in PBS containing 0.1% Tween 20 (PBST)]. Membranes were incubated with the rabbit polyclonal R6 antiserum against relaxin diluted 1:2500 in blocking solution overnight at 4°C, then washed in PBST and incubated with the secondary goat anti-rabbit at 1:20,000 in blocking buffer for 1 hour at room temperature before immunodetection with the ECL kit (Amersham). For the detection of cathepsins, cells were isolated in 2× extraction buffer under reducing conditions [125 mmol/L Tris-HCl, pH 6.8, 4% SDS, 20% glycerol, 10% mercaptoethanol (ME); 2% bromophenol blue; all reagents from Sigma]. Supernatants containing secreted cathepsins were collected from a confluent cell layer cultured in medium plus 2.5% FCS after 72 hours and centrifuged at 4000 × *g* for 30 minutes at 4°C to pellet remaining cells. Equal volumes of the supernatants and 2× extraction buffer were mixed and protein extracts of both cellular and soluble fractions (40 μl each) were separated on a reducing 12% SDS-polyacrylamide gel

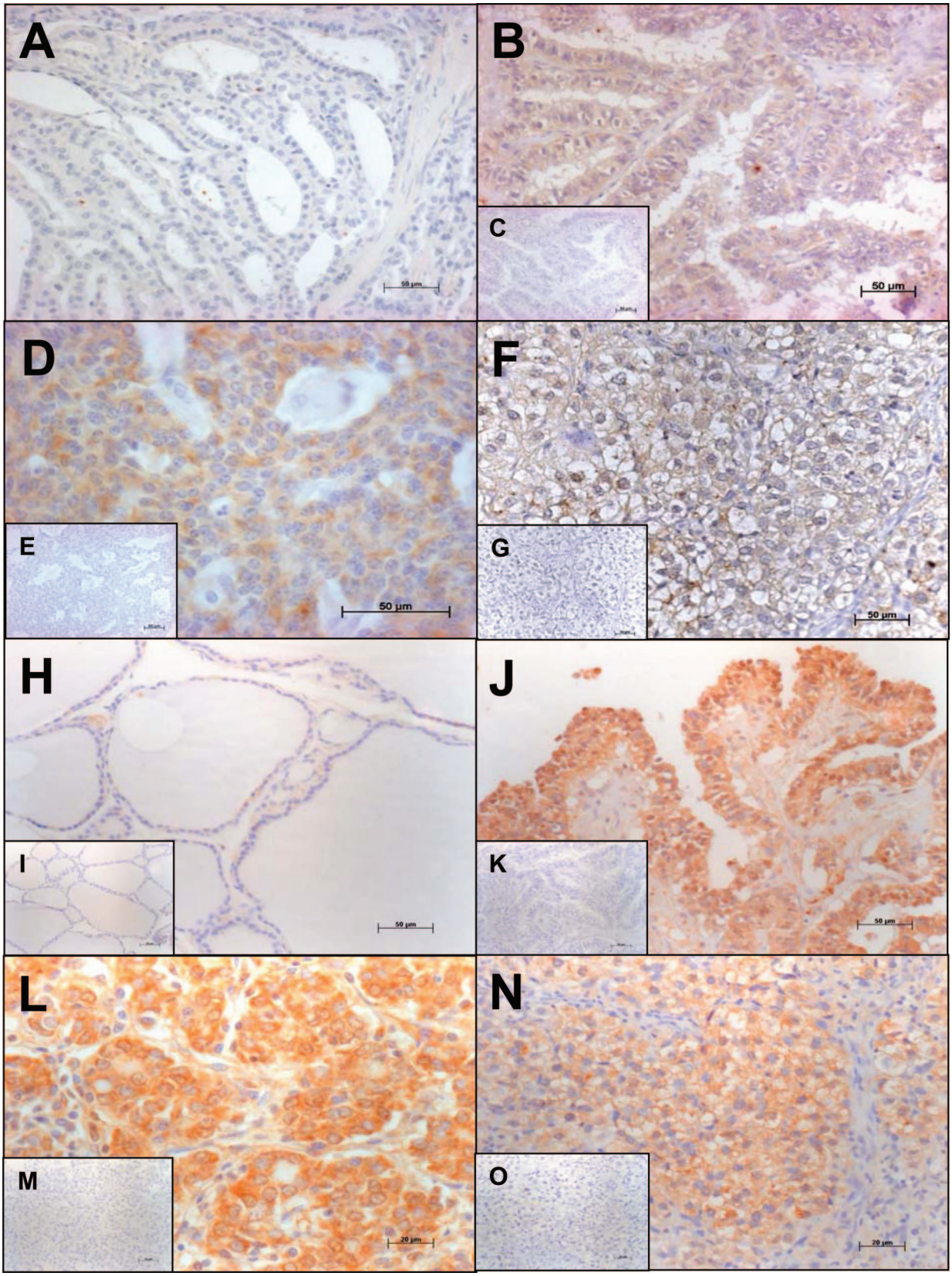

Figure 1. Immunolocalization of RLN2 and LGR7. Human goiter (**A**) and Graves' disease (not shown) tissues were devoid of RLN2. By contrast, RLN2 immunoreactivity was present in human papillary (PTC; **B**), follicular (FTC; **D**), and dedifferentiated, anaplastic thyroid carcinoma (UTC; **F**). **H:** Using a previously characterized rabbit polyclonal antiserum to human LGR7,[8] weak immunoreactivity for LGR7 was detected in thyrocytes of normal human thyroid tissues. Irrespective of pTNM classification of the tumor tissues investigated, immunoreactive LGR7 was up-regulated in PTC (**J**), FTC (**L**), and UTC (**N**) tissues (Table 1). Sections incubated with a rabbit nonimmune serum as control were devoid of immunostaining as demonstrated by the representative **insets** (**C**, **E**, **G**, **I**, **K**, **M**, **O**). Original magnifications: ×200 (**A–C**, **E**, **H–K**, **M**); ×400 (**D**, **F**, **G**, **L**, **N**, **O**).

electrophoresis. After protein transfer and blocking of nonspecific binding sites for 2 hours with 5% skimmed milk in PBST, membranes were incubated overnight at 4°C with the rabbit polyclonal antibodies to cath-D (1:7500),[22] cath-B (both 1:500), and cath-H (1:10,000) and mAbs to cath-K (1:200), cath-V (1:500). Also, we used the two mAbs specific for procath-L (2D4 at 1:500) and all three cath-L forms (33/1 at 1:500),[23,24] respectively. Secondary horseradish peroxidase-conjugated goat anti-rabbit and rabbit anti-mouse Igs were used at 1:20,000 for 1 hour at room temperature, respectively. Membranes were washed and immunoreactive proteins were visualized with the ECL kit (Amersham). In all cases, β-actin was used to determine equal protein loading. Membranes were incubated in stripping solution (2% SDS, 125 mmol/L Tris-HCl, pH 8.0, 0.7% ME), blocked and incubated at 1:20,000 in blocking buffer for 1 hour each with a mAb to human β-actin (Sigma) and the secondary goat anti-mouse, respectively, before immunodetection with the ECL kit (Amersham).

Statistical Analysis

Statistical analysis was performed with the SPSS software package (SPSS GmbH, Munich, Germany). Student's *t*-test and one-way analysis of variance were used. All experiments were performed at least in triplicates and were expressed as mean ± SEM with P values of $P < 0.05$ considered as statistically significant.

Results

RLN2 and LGR7 Relaxin Receptor in Human Thyroid Tissues

RT-PCR analysis of the human thyroid tissues investigated (Table 1) revealed the expression of *RLN2* and *LGR7*. *RLN2* transcripts were detected in 12 of 14 (86%) papillary thyroid carcinoma (PTC), 10 of 12 (83%) follicular thyroid carcinoma (FTC), and 13 of 14 (93%) undifferentiated thyroid carcinoma (UTC) tissues, respectively (Table 1). *LGR7* transcripts were demonstrated in 12 of 14 (86%) PTC and in 100% of FTC and UTC tissues tested (data not shown). Goiter and Graves' disease tissues investigated did not express *RLN2* transcripts. Goiter and Graves' disease tissues and thyroid tissue sections with the primary antiserum omitted were also devoid of RLN2 immunostaining (Figure 1, A, C, E, and G). Similar to the RT-PCR data, immunoreactive RLN2 was exclusively detected in the human PTC, FTC, and UTC investigated (Figure 1, B, D, and F; Table 1). Independent of pTNM classification, the presence of immunostained RLN2 was moderate in PTC/FTC and moderate to high in UTC. Similar results for the immunodetection of RLN2 in serial tissue sections were obtained with either the R6 antiserum or the anti-RLN2 serum from Immundiagnostik[21] (data shown for the latter relaxin antiserum).

A single *LGR7* transcript was detected in all human thyroid tissues investigated (data not shown). Weak immunoreactive LGR7 was detected in all human thyroid tissues of goiter (Figure 1H) and Graves' disease. Moderate to high immunoreactive LGR7 was detected in all human thyroid carcinoma tissues investigated (Figure 1, J, L, and N). Thyroid tissue sections with the primary antiserum omitted were devoid of specific LGR7 immunostaining (Figure 1, I, K, M, and O).

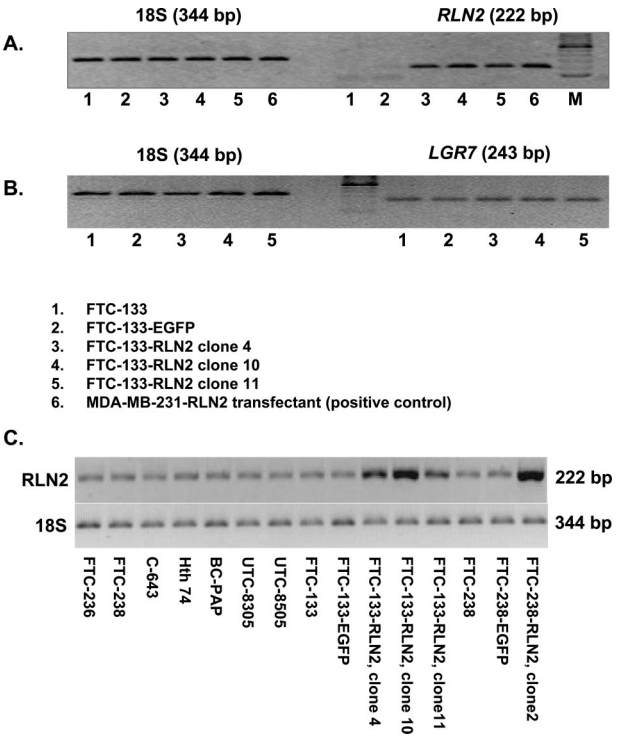

Figure 2. A: Representative RT-PCR of a specific 222-bp pro*RLN2* amplicon in stable FTC-133-RLN2 transfectants (**lanes 3** to **5**), an FTC-133-EGFP control clone (**lane 2**), and untransfected FTC-133 (**lane 1**). MDA-MB-231 human mammary carcinoma cell transfectant overexpressing proRLN2 relaxin served as positive control (A6).[59] **B:** Amplification of 18S transcripts was used to ensure loading of equal cDNA amounts for semiquantitative RT-PCR. RT-PCR amplifications of *LGR7* transcripts are shown for FTC-133 (**lane 1**), FTC-133-EGFP control (**lane 2**), and the FTC-133-RLN2 transfectants (**lanes 3** to **5**). Comparative analysis of RLN2 transcriptional gene activity in eight established human thyroid carcinoma cell lines and the stable FTC-133 and FTC-238 transfectants investigated. **C:** The human thyroid carcinoma cell lines BC-PAP, UTC-8305, UTC-8505, and C643 demonstrated increasing *pro-RLN2* expression in ascending order. Strongest expression of *RLN2* amplicons was observed in all RLN2 stable transfectants.

Stable Transfectants of Human Thyroid Carcinoma Cells Produce Bioactive Relaxin

Human thyroid carcinoma cell lines were investigated for transcriptional gene activity of *RLN2* and *LGR7* (Figure 2, A–C). All follicular thyroid carcinoma cell lines, FTC-133, FTC-236, and FTC-238, and the anaplastic, undifferentiated thyroid carcinoma cell lines Hth74, UTC-8305, UTC-8505, and C643 weakly expressed transcripts encoding *RLN2* when 2 μl of cDNA were used in the PCR reaction (Figure 2C). These cell lines also expressed *LGR7* transcripts at low levels (data not shown). FTC-133 expressed *LGR7* transcripts. However, endogenous *RLN2* expression was only detected at higher cDNA concentration (2 μl/tube) in each PCR reaction (Figure 2C), but was not detectable when 1 μl of cDNA was used in the

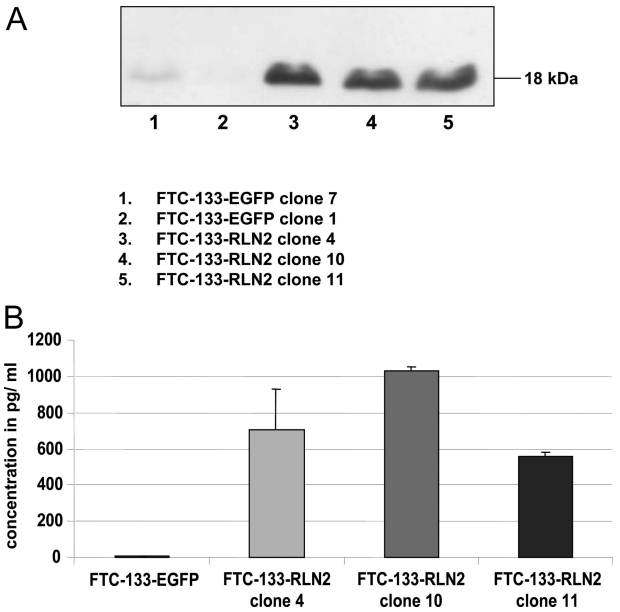

Figure 3. A: Representative Western blot analysis revealed an immunoreactive product resembling proRLN2 relaxin in size (18 kd) produced exclusively by the FTC-133-RLN2 (**lanes 3** to **5**) but not by FTC-133-EGFP transfectants (**lanes 1** and **2**). Similar RT-PCR and Western blot results were obtained for the FTC-238-RLN2 clones (not shown). Membranes were stripped and reprobed with an antibody to β-actin to demonstrate equal protein loading (not shown). **B:** Representative RLN2-ELISA of a confluent layer of FTC-133-RLN2 transfectants after 48 hours of culture. The amount of secreted relaxin ranged from 580 to 1050 pg/ml, maximally 95-fold higher as with a FTC-133-EGFP clone that secreted negligible levels of relaxin and served as a negative control in the RLN2-ELISA. FTC-238-RLN2 transfectants demonstrated an ~70-fold increase in relaxin secretion (data not shown).

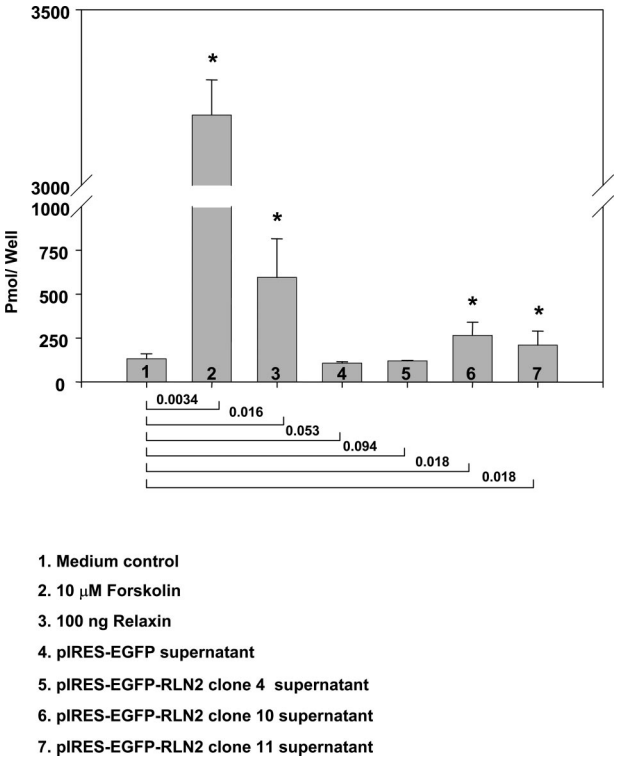

Figure 4. Representative result from cAMP enzyme immunoassay assays with the responder transfectant FTC-133-RLN2, clone 10, incubated for 1 hour with supernatants derived from FTC-133-EGFP (negative control) and different FTC-133-RLN2 transfectants. Exposure to 10 μmol/L forskolin as a positive control resulted in a highly significant increase in cAMP levels indicating the presence of a functional adenylate cyclase system in FTC-133. *P* values were calculated in relation to cAMP values obtained from the responder cells exposed to normal culture medium as negative control and are shown for each comparison below the graph; a $P < 0.05$ was considered significant (asterisk).

PCR reaction (Figure 2A). We chose FTC-133 and FTC-238 for stable transfection with the pCMV-preproRLN2-IRES-EGFP construct. The FTC-133-RLN2 stable transfectants overexpressed relaxin transcripts as determined by RT-PCR analysis (Figure 2A). Western blot analysis revealed a single specific immunoreactive band at ~18 kd corresponding to proRLN2 relaxin, which was very weak in EGFP clones (Figure 3A). The amounts of relaxin secreted by the FTC-133-RLN2 transfectants (580 to 1050 pg/ml) was maximally 95-fold that of corresponding EGFP controls that produced small levels of immunoreactive relaxin as calculated with a relaxin standard in an RLN2 ELISA (Figure 3B). Similar results were obtained for FTC-238-RLN2 stable transfectant that produced ~70-fold higher levels of relaxin (730 pg/ml) as compared to corresponding EGFP controls with low levels of relaxin (data not shown).

FTC-133-RLN2 and FTC-133-EGFP transfectants contained a functional adenylyl cyclase system that responded to forskolin treatment with high cAMP levels (Figure 4). Supernatants derived from the FTC-133-RLN2 clones 4, 10, and 11 caused a weak but specific increase in intracellular cAMP in FTC-133 clone 10 that was used as responder cell line in this assay (Figure 4). The increase in cAMP levels was highest with supernatant from a 24-hour culture of FTC-133-RLN2, clone 10, and this clone also showed the strongest production of relaxin in the RLN2-ELISA (Figure 3B). FTC-133-RLN2 transfectants displayed enhanced metabolic activity and enhanced mitochondrial activity reflected by the increased formation of $NADH_2$-dependent formazan salt in the MTT cell viability assays (Figure 5A) and elevated intracellular ATP levels (Figure 5B). Suppression of *LGR7* expression by *LGR7* siRNA treatment of FTC-133 abolished the enhanced MTT response on incubation with recombinant RLN2 (data not shown). Overexpression of RLN2 failed to result in a significant increase in cell proliferation as determined by nonradioactive BrdU proliferation assays (Figure 5C). FTC-238-RLN2 clones did not display altered MTT or ATP values as compared to FTC-238-EGFP controls (data not shown). This may indicate cell-type-specific RLN2-induced and LGR7-mediated metabolic changes among human follicular thyroid carcinoma cells.

Relaxin Enhances Anchorage-Independent Growth and Increases Motility and Migration through Elastin Matrices by Human Thyroid Carcinoma Cells

Soft agar assays were performed with FTC-133-RLN2 and FTC-133-EGFP transfectants. Relaxin significantly enhanced the numbers of colonies (maximum eight-fold) during anchorage-independent growth of FTC-133-RLN2 clones as compared to FTC-133-EGFP con-

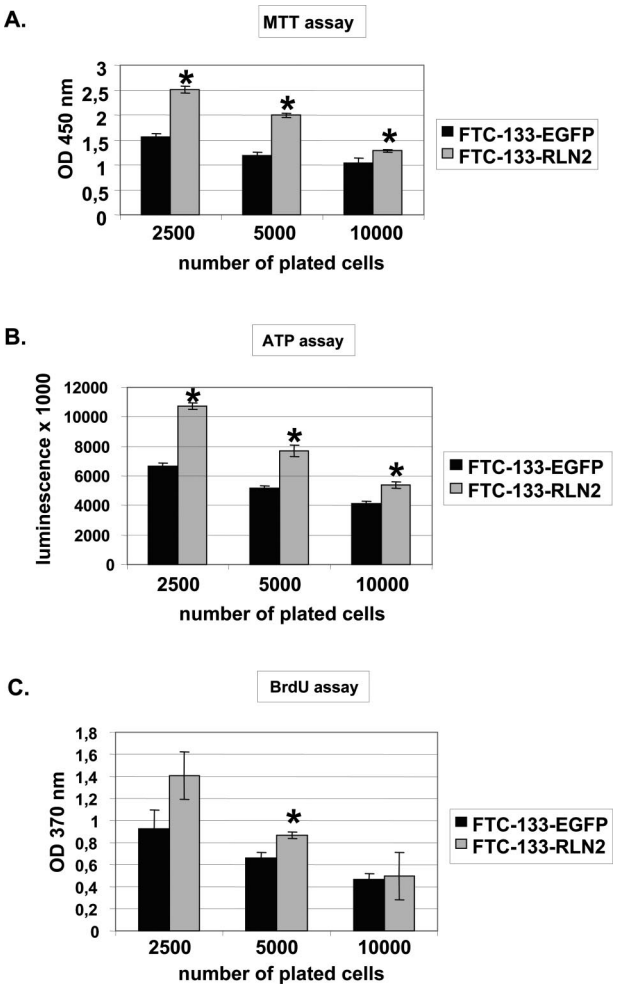

Figure 5. A: FTC-133-RLN2 transfectants (gray columns) displayed significantly (asterisk) increased $NADH_2$-dependent production of formazan salts after 6-hour incubations compared to FTC-133-EGFP controls (black columns). **B:** Also reflecting enhanced mitochondrial activity, increased intracellular ATP levels were determined in the FTC-133-RLN2 clones at all cell densities investigated. Nonradioactive BrdU proliferation assays of FTC-133 transfectants revealed a small but significant (asterisk) increase in proliferation rates by FTC-133-RLN2 when seeded at lower cell numbers (0.5×10^4 cells with $P \leq 0.005$). A statistically less significant ($P \leq 0.01$) increase in proliferation was observed with 0.25×10^4 cells per well. **C:** The proliferative response to relaxin was diminished at high cell numbers (10^4 cells) indicating that RLN2 did not act as a strong mitogen on FTC-133. All data from these three assays were normalized to 0.5×10^4 cells.

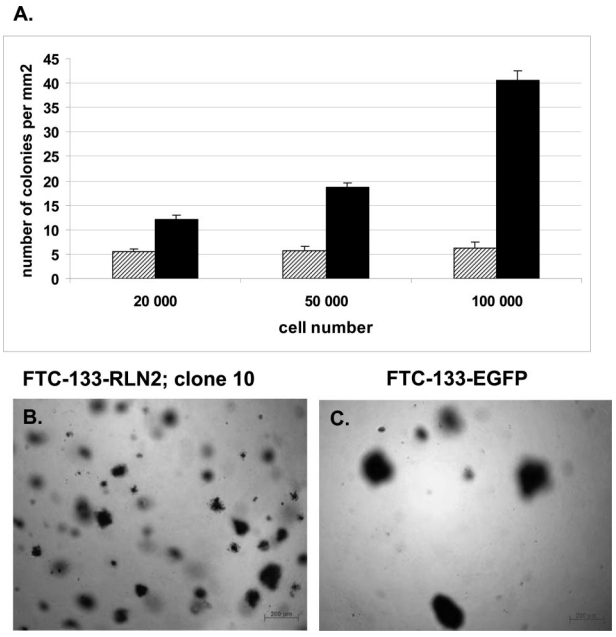

Figure 6. A: Representative soft agar colony assay for FTC-133-RLN2 clone 10 revealed an up to eight times higher number of colonies formed by FTC-133-RLN2 transfectants (black columns) as compared to the FTC-133-EGFP controls (gray columns). In addition, the colonies formed by the relaxin-secreting FTC-133 transfectants were smaller and more disseminated throughout the soft agar (**B**) as compared to EGFP controls (**C**). The number of cell colonies is represented as means of the counting results from 10 different areas.

trols (Figure 6A). FTC-133-RLN2 transfectants (Figure 6B) generated smaller-sized colonies when compared to EGFP controls (Figure 6C). RLN2 significantly enhanced the motility of human thyroid carcinoma cells as determined in filter-based motility assays using recombinant RLN2 and RLN2 secreted by the stable transfectants. The motility-promoting action of RLN2 was unaffected by FCS. The paracrine actions of recombinant RLN2 caused a significant concentration-dependent increase in the motility of FTC-133 (Figure 7A) and FTC-238 cells (data not shown). In addition, RLN2 transfectants of both FTC-133 (Figure 7B) and FTC-238 (Figure 7C) plated onto the filter displayed enhanced cellular motility as compared to corresponding EGFP controls. When the FTC-133-RLN2 transfectants were also present in the lower chamber an additive autocrine/paracrine effect of RLN2 on the motility was observed for all RLN2-transfectants seeded on top of the filter as depicted for FTC-133-RLN2 clone 10 (Figure 7B). In addition, secreted relaxin from the FTC-133-RLN2 transfectants in the lower chambers also resulted in an increased number of FTC-133-EGFP clones to traverse the filter from the upper chamber (Figure 7B). To determine the ability of FTC-133-RLN2 clones to actively penetrate an extracellular matrix, we performed migration assays using filters coated with elastin. FTC-133-RLN2 transfectants displayed a 4.5-fold increased rate of migration through an elastin matrix as compared to EGFP control cells indicating a novel role for relaxin in enhancing the elastinolytic activity of human thyroid carcinoma cells (Figure 7D). This relaxin-mediated increased elastinolytic activity was also shown for FTC-238 carcinoma cells exposed to human recombinant RLN2 and for FTC-238-RLN2 transfectants resulting in increased migration through elastin matrices (Figure 7E).

Impaired RLN Signaling Decreases the Invasive Potential of Human Thyroid Carcinoma Cells

The specificity of RLN2-induced enhanced migration of human thyroid carcinoma cells was demonstrated by heat inactivation or dilution of RLN2 ligand. Heat-inactivated RLN2 was unable to enhance the motility of thyroid carcinoma cells (Figure 8A; black columns). Also, RLN2-mediated enhanced motility of FTC-133 was concentration-dependent as demonstrated by the inability of higher dilutions

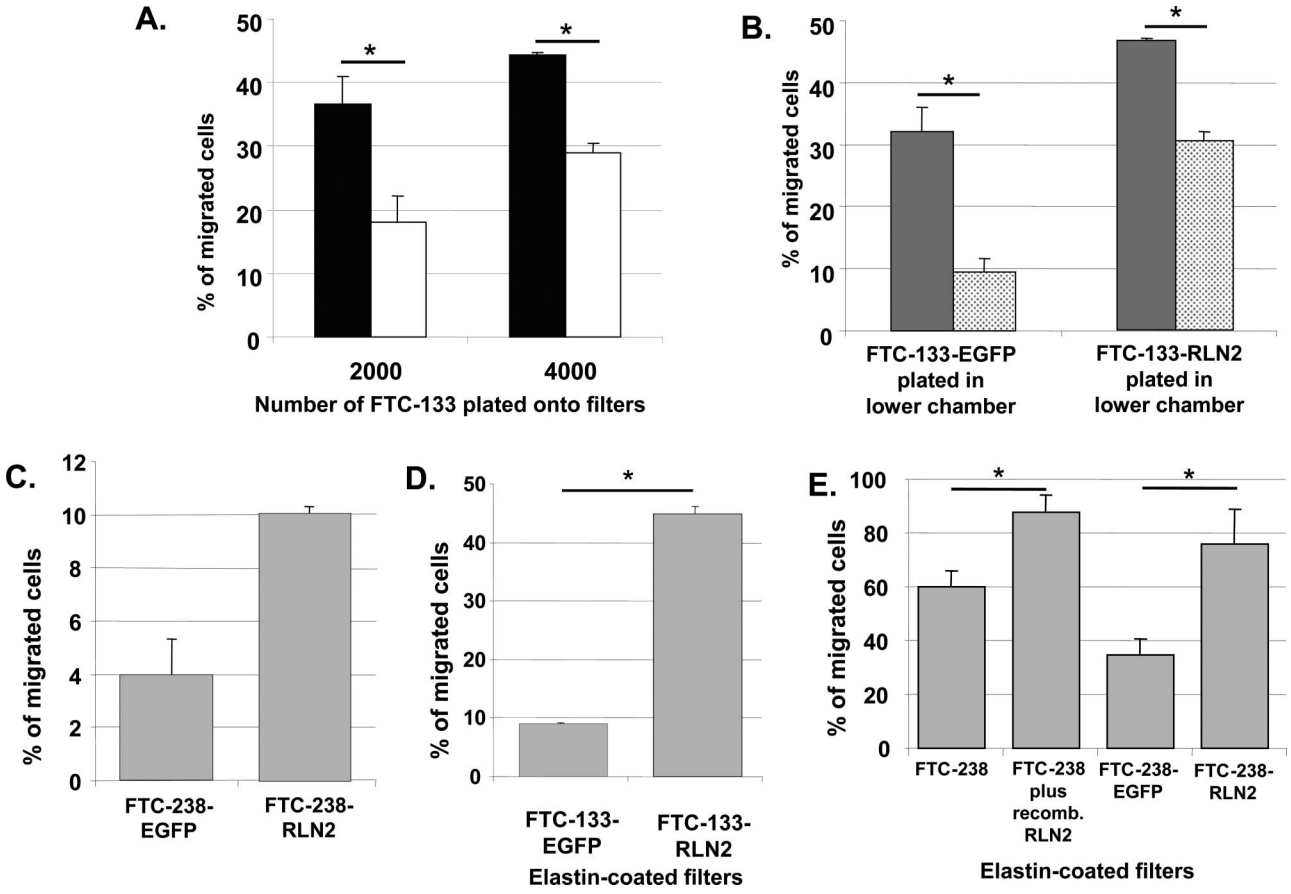

Figure 7. A: In a two-chambered motility assay, untransfected FTC-133 exposed to 100 ng/ml of recombinant RLN2 (black column) showed significantly increased motility when compared with untreated FTC-133 (white column) as determined by the number of cells that had traversed the 8-μm filter pores. **B:** Enhanced motility was also observed with FTC-133-RLN2 transfectants (gray column) as compared to FTC-133-EGFP controls (dotted column). A paracrine motility-promoting effect was observed for the FTC-133-RLN2 (gray column) and FTC-133-EGFP clones (dotted column) when relaxin-secreting FTC-133-RLN2 transfectants (5×10^4 cells) were additionally plated into the lower chamber. This paracrine effect was absent when FTC-133-EGFP (5×10^4) cells were plated in the lower chamber. **C:** FTC-238-RLN2 transfectants also showed enhanced motility as compared to FTC-238-EGFP controls. **D:** Migration assays through elastin-coated filters demonstrated an ~4.5-fold enhanced migration of the FTC-133-RLN2 transfectants as compared to the FTC-133-EGFP controls indicating relaxin-mediated enhanced elastinolytic activity in these FTC-133-RLN2 transfectants. **E:** RLN2 also increased the elastinolytic activity in FTC-238 as shown for FTC-238 treated with recombinant RLN2 and for stable FTC-238-RLN2 transfectants.

of supernatants from a relaxin-secreting FTC-133-RLN2 transfectant (clone 10) to increase the motility of FTC-133 (Figure 8A; gray columns). An intact LGR7 receptor signaling system was identified as a pathway for the specific RLN2-mediated promigratory action in human thyroid carcinoma cells. Specific siRNA-*LGR7* treatment was used to suppress LGR7 signaling. We used a single siRNA construct targeting exon 15 of the human *LGR7* mRNA that effectively decreased the relative amount of *LGR7* transcripts by half in FTC-133 cells as determined by semiquantitative RT-PCR (Figure 8B). Suppression of *LGR7* transcript levels in FTC-133 was associated with a significant reduction in cAMP response (Figure 8C) and decreased tumor cell motility (Figure 8D), effectively rendering these human thyroid carcinoma cells nonresponsive to RLN2. To exclude a nonspecific inhibitory effect of the single siRNA construct used at 300 nmol/L, we used a set of two additional LGR7 siRNAs at 50 nmol/L each (total 100 nmol/L), targeting sequences located in exons 4 and 20 of *LGR7*. We observed a significant reduction in the motility of FTC-133 and FTC-238 on treatment with 100 or 500 ng/ml of relaxin respectively (data not shown). Thus, the RLN2-LGR7 ligand-receptor signaling system is an important novel mediator of thyroid carcinoma invasiveness.

Relaxin Stimulates the Production, Secretion, and Intracellular Distribution of Cathepsins in Human Thyroid Carcinoma Cells

Cathepsins are lysosomal acid hydrolases, and some members possess elastinolytic activity.[25] We investigated the production of six cathepsins (cath-B-, D, -H, -L, -K, -V) in cellular and secreted protein fractions of RLN2 and EGFP clones from FTC-133 and FTC-238. Western blot analysis revealed that all FTC-133 transfectants were devoid of immunoreactive cath-B, -H, -K, and -V but produced cath-D and elastinolytic cath-L immunoreactive forms. The mAb 2D4 specifically detected the proform (42 kd) as a cellular and secreted cath-L form (Figure 9A). Also, using mAb 33/1 the three known immunoreactive forms of cath-L resembling the proform (42 kd), single-chain (31 kd), and heavy chain (24 kd) of the two-chain cath-L were detected in cellular protein ex-

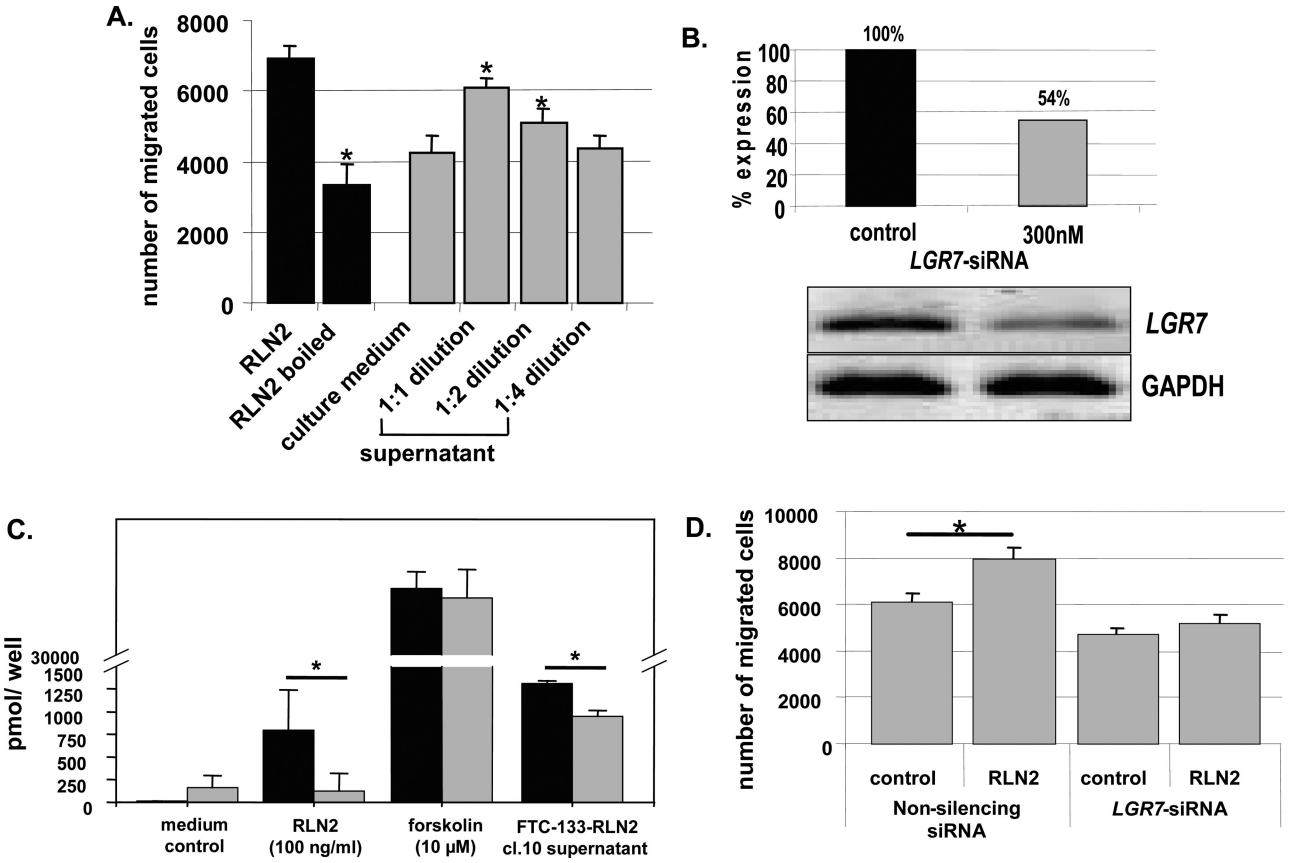

Figure 8. The specificity of the RLN2-LGR7 signaling in mediating the described tumor-promoting activity of RLN2 was shown by reducing the amount of bioactive RLN2 ligands (**A**) and by decreasing the number of *LGR7* transcripts using a specific siRNA-*LGR7* construct (**B–D**). **A:** Heat-inactivation of 500 ng/ml of RLN2 significantly decreased cellular motility (black columns). Dilution of culture supernatants from FTC-133-RLN2 transfectants also revealed a clear concentration-dependent decrease in motility of FTC-133 (gray columns). FTC-133 exposed to normal culture medium served as negative control. **B:** After 3 days of incubation with a specific siRNA-*LGR7* at 300 nmol/L, FTC-133 displayed an ~50% reduction in *LGR7* transcripts. **C:** These siRNA-*LGR7*-treated FTC-133 cells (gray columns) displayed a significant reduction in cAMP response on stimulation with either recombinant human RLN2 or supernatants derived from FTC-133-RLN2 (clone 10) as compared to FTC-133 transfected with the nonsilencing siRNA construct (black columns). **D:** Nonsilencing siRNA also failed to inhibit the motility-promoting effect of recombinant RLN2 when compared to control cells not exposed to recombinant RLN2. FTC-133 and FTC-238 (not shown) treated with the siRNA-*LGR7* did not elicit increased motility in the presence of exogenous RLN2. Thus, the cAMP response toward RLN2 and the motility-enhancing action of (pro)RLN2 were both mediated by the LGR7 signaling pathway in FTC-133 human thyroid carcinoma cells.

tracts (Figure 9B). FTC-133-RLN2 clones consistently displayed an up-regulation of the heavy chain cath-L (24 kd) in cellular extracts suggesting complete processing of cath-L in these clones. Procath-L (42 kd), single-chain (31 kd), and heavy chain cath-L immunoforms were also identified as a secretion product of FTC-133 transfectants with the amount of heavy chain cath-L secreted by FTC-133-RLN2 clones being consistently higher as compared to FTC-133-EGFP transfectants (Figure 9B). Immunoreactive 25-kd and 52-kd cath-D, resembling the heavy chain and proenzyme, were detected in cellular extracts of the FTC-133-RLN2 clones (Figure 9C). Production of procath-D (52 kd) was enhanced and that of cath-D heavy chain (25 kd) decreased as compared to EGFP controls. Procath-D was the only secreted cath-D form detected in all FTC-133-clones (Figure 9C). Similar changes in the production and secretion of cath-L (Figure 9D) and cath-D forms (data not shown) were observed in FTC-238-RLN2 transfectants as compared to FTC-238-EGFP controls suggesting that these alterations are part of a common RLN2-mediated response in human thyroid carcinoma cells. The mAbs 2D4 and 33/1 used to immunolocalize human procath-L and all three forms, procath-L, single chain, and heavy chain form, respectively, gave similar results in RLN2 and EGFP transfectants of FTC-133 and FTC-238.

Immunofluorescence imaging revealed the intracellular distribution of immunoreactive procath-L to be significantly altered in proRLN2 transfectants as demonstrated for FTC-133 (Figure 10, B and C) and FTC-238 (data not shown) when compared with corresponding EGFP controls (Figure 10A) or normal FTC-133 and FTC-238 (data not shown). mAb 33/1 revealed a similar perinuclear to polar cytosolic distribution of cath-L forms in RLN2 transfectants (Figure 10, E and F) as compared to a diffuse cytoplasmatic cath-L immunostaining in EGFP clones (Figure 10D). Confocal laser-scanning microscopy confirmed the perinuclear immunolocalization of cath-L exclusively in RLN2 transfectants and revealed the presence of nuclear cath-L in both FTC-133-RLN2 and FTC-133-EGFP transfectants (Figure 10G). By contrast, no differences in the exclusively cytoplasmic distribution were observed with the polyclonal anti-cath-D antiserum

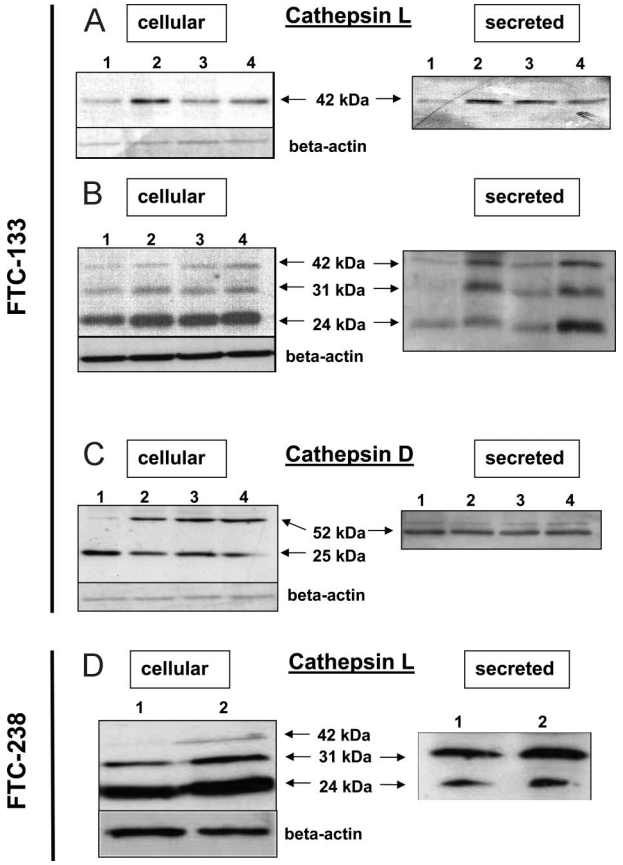

Figure 9. Western blot analyses for cellular and secreted cath-L and cath-D from FTC-133-EGFP (**A–C**, **lanes 1**) and different FTC-133-RLN2 transfectants (**A–C**, **lanes 2** to **4**). **B:** Immunoreactive forms at 24, 31, and 42 kd resembling the heavy chain, single chain, and procath-L, respectively, were detected with the mAb 33/1[23,24] in the cellular and secreted protein fractions of all FTC-133 transfectants investigated. When compared with FTC-133-EGFP clones (**A** and **B**, **lanes 1**), FTC-133-RLN2 (**A** and **B**, **lanes 2** to **4**) displayed increased production and secretion of the cath-L proform (42 kd) as determined by the mAb 2D4[22] specific for procath-L (**A**) and the mAb 33/1[23,24] against an epitope present in all three cath-L forms (**B**). **B:** In addition, FTC-133-RLN2 clones (**lanes 2** to **4**) showed enhanced production and secretion of the 31-kd and 24-kd bioactive cath-L forms as compared to FTC-133-EGFP clones (**lane 1**). **C:** Two immunoreactive cath-D forms at 52 kd and 25 kd were detected in the cellular protein fractions of both FTC-133-EGFP (**lane 1**) and FTC-133-RLN2 (**lanes 2** to **4**) transfectants. FTC-133-RLN2 displayed significantly increased amounts of procath-D at 52 kd in cellular extracts (**lanes 2** to **4**) as compared to FTC-133-EGFP controls (**lane 1**). The amount of the 25-kd cath-D in the cellular extracts was slightly reduced in all FTC-133 clones studied (**lanes 1** to **4**). The secreted protein fraction exclusively contained procath-D (52 kd) at similar levels in FTC-133-EGFP (**lane 1**) and FTC-133-RLN2 (**lanes 2** to **4**) transfectants. Equal protein loading was checked by β-actin staining of stripped membranes. **D:** Representative Western blots are shown for cellular and secreted cath-L of FTC-238-EGFP (**lane 1**) and FTC-238-RLN2 clones (**lane 2**). Similar to FTC-133-RLN2 clones, corresponding FTC-238-RLN2 transfectants demonstrated an up-regulation in cath-L single chain (31 kd) and heavy chain (24 kd), whereas the amount of procath-L (42 kd) produced by the FTC-238 clones was negligible. The pattern of cellular and secreted cath-D in the FTC-238-RLN2 transfectant was similar to corresponding FTC-133 clones (data not shown).

for FTC-133-EGFP (Figure 10H) and FTC-133-RLN2 transfectants (Figure 10I).

Vesicular transport of mannose-6-phosphate-tagged cathepsins from the Golgi to the lysosomes is facilitated by mannose-6-phosphate receptor. RLN2 clones displayed a cytoplasmic perinuclear distribution of immunoreactive mannose-6-phosphate receptor (Figure 10K) similar to that observed for (pro)cath-L (Figure 10, B and C). By contrast, a diffuse cytosolic immunodistribution was observed in EGFP transfectants (Figure 10J). Lysosomal CD63 marker did not reveal differences in cellular distribution among transfectants as shown for one FTC-133-RLN2 clone (Figure 10L).

Discussion

We have identified human thyrocytes of primary and metastatic thyroid carcinoma tissues, but not normal and hyperplastic thyrocytes, as a novel source of RLN2. The detection of *LGR7* relaxin receptor, mRNA, and immunoreactive protein, in normal and neoplastic thyrocytes of patient tissues confirmed and extended a previous report on the expression of *LGR7* mRNA[8] in the human thyroid and identified human thyroid neoplastic lesions as a target for the autocrine/paracrine actions of relaxin. Neoplastic thyrocytes are not the only source of relaxin in the human thyroid because we recently detected RLN2 as an early product of neoplastic interstitial C cells during medullary thyroid carcinogenesis.[18] Relaxin's actions in human thyroid carcinoma may be complex and mediated by both LGR7 and the relaxin/INSL3 receptor LGR8 as suggested by the detection of *LGR8* transcripts in both the human thyroid gland and human thyroid carcinoma cell lines.[8,13] We also previously reported the presence of relaxin-like INSL3 in hyperplastic human thyrocytes of Graves' disease and neoplastic thyrocytes.[13] The differences in thyroidal expression pattern between relaxin and INSL3 implicate distinct functional roles for each of the relaxin-like members in the human thyroid and evidence in mice suggests that relaxin and INSL3 appear to activate distinct LGR7- and LGR8-mediated signaling pathways, respectively.[26]

Stable transfectants of the relaxin-responsive human follicular thyroid carcinoma cell lines FTC-133 and FTC-238 were used to analyze functional roles of RLN2 in human neoplastic thyrocytes. These transfectants produced a single proRLN2 immunoprotein indicating incomplete processing of RLN2 hormone in these thyroid carcinoma cells likely reflecting their limited capacity to process constitutively produced relaxin proform. Another explanation may be that human neoplastic thyrocytes generally have a limited capability to properly process relaxin-like members because we also detected proINSL3 as the main product in human thyroid carcinoma tissues.[13] As shown in other cell models, proRLN2 was bioactive and specifically activated LGR7 receptors.[15,27–29] Down-regulation of *LGR7* gene expression with an *LGR7* siRNA construct caused a statistically significant reduction in cAMP response on stimulation of cells with either recombinant RLN2 or RLN2-containing supernatants derived from FTC-133-RLN2 secreting transfectants demonstrating predominantly LGR7-mediated RLN2 signaling pathways in these thyroid carcinoma cells.

Among the specific relaxin-mediated effects was a novel role of RLN2 as modulator of metabolic activity causing enhanced mitochondrial activity and increased intracellular ATP production in the FTC-133-RLN2 clones.

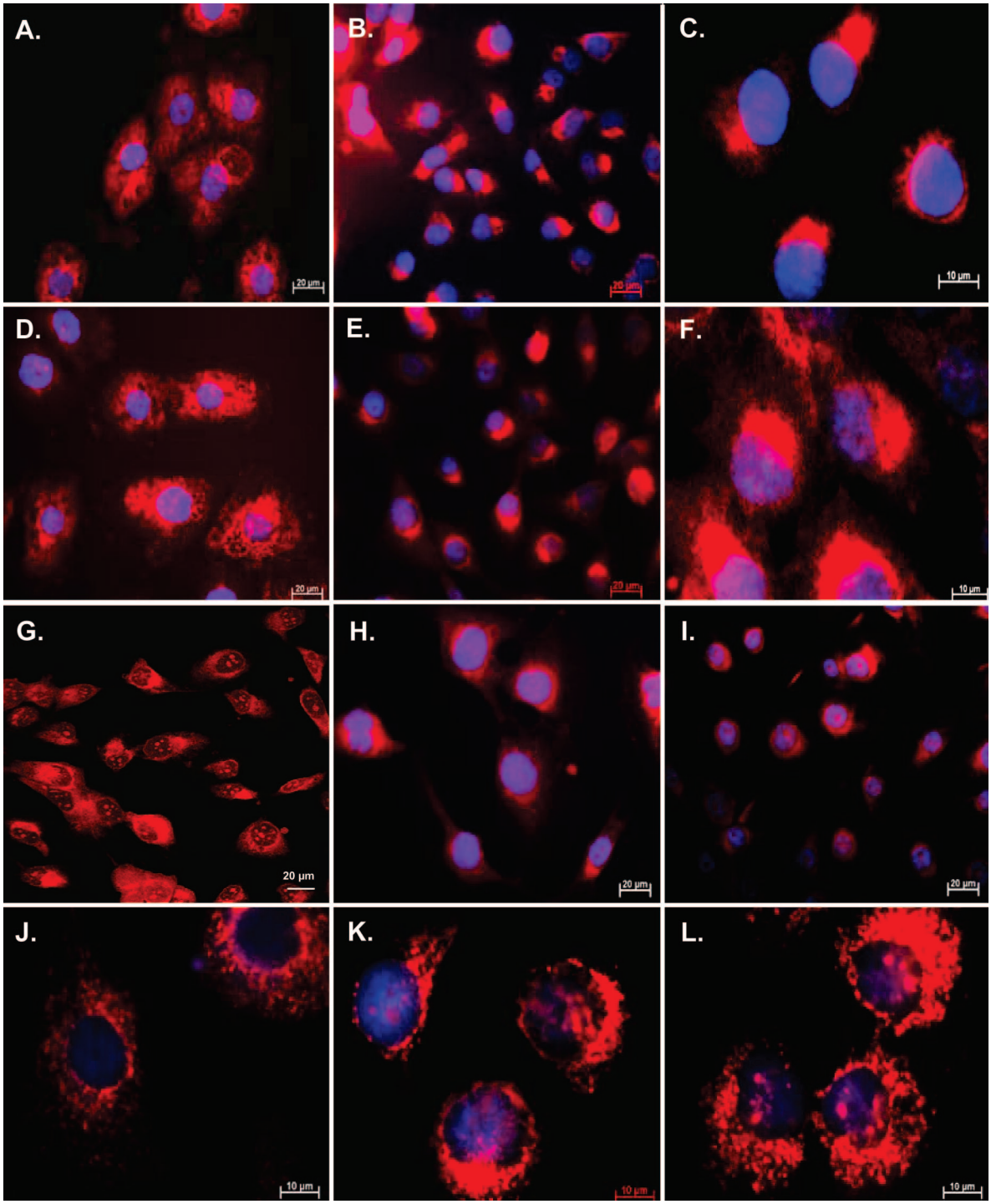

Figure 10. **A:** Immunofluorescent detection of human procath-L using the mAb 2D4 specific for human procath-L[22] revealed randomized cytoplasmic immunostaining in FTC-133-EGFP clones. **B**, **C:** By contrast, a perinuclear and polar distribution of immunoreactive procath-L was observed in the FTC-133-RLN2 transfectants. Using the mAb 33/1 recognizing a common epitope in all three known human cath-L forms,[23,24] FTC-133-EGFP clones (**D**) displayed a similar cytoplasmic immunostain as observed with the procath-L mAb 2D4 (**A**). **E** and **F:** FTC-133-RLN2 clones and FTC-238-RLN2 transfectants (not shown) showed a localized perinuclear distribution and cytoplasmic immunostain of cath-L. **G:** Confocal microscopy confirmed the perinuclear localization of cath-L in RLN2 transfectants only and revealed immunoreactive cath-L in the nucleus of FTC-133-RLN2 and FTC-133–EGFP transfectants (not shown). **H** and **I:** Cath-D was detected as a cytosolic immunoprotein with no apparent differences in the distribution between FTC-133-EGFP-transfectants (**H**) and FTC-133-RLN2 clones (**I**). Immunofluorescent detection of mannose-6-phosphate receptors in FTC-133-EGFP controls (**J**) showed a cytoplasmic granular stain, whereas a distinct polar to perinuclear distribution resembling the distribution of procath-L (**C**) was observed in FTC-133-RLN2 (**K**). **L:** Both FTC-133-RLN2 and FTC-133-EGFP clones showed a similar granular cytoplasmic immunostaining for the lysosmal marker CD63. Original magnifications: ×400 (**A**, **B**, **D**, **E**, **G–I**); ×1000 (**C**, **F**, **J–L**).

A protective role of relaxin in mitochondria was demonstrated in guinea pig cardiomyocytes exposed to hypoxic conditions, which was associated with an ability of relaxin to prevent mitochondrial membrane breakdown and sustain mitochondrial integrity under hypoxia.[30] Similar to a recent report on relaxin in endometrial cancer,[31] relaxin failed to act as a potent mitogen in thyroid carcinoma cells. Instead, increased cellular viability and enhanced tumor cell survival appeared to be important relaxin-mediated actions on neoplastic thyrocytes as reflected by the large number of disseminated small-sized colonies during anchorage-independent growth of the FTC-133-RLN2 transfectants.

Activating LGR7 signaling cascades, relaxin affected the migratory behavior of human neoplastic thyrocytes. Relaxin has previously been identified as a hormone promoting the motility of human and canine mammary carcinoma cell lines (human, MCF-7 and SK-BR3; canine, CF33.Mt)[15,32] as well as noncarcinogenic bronchial epithelial cells and inflammatory cells infiltrating wounds.[33,34] Here we demonstrate that both recombinant RLN2 and secreted proRLN2 profoundly accelerated the cellular motility of two human thyroid carcinoma cell lines (FTC-133 and FTC-238) and the corresponding RLN2 transfectants in an autocrine/paracrine LGR7-dependent manner. The ability to promote tumor cell motility appears to be characteristic for both relaxin members, relaxin and INSL3, because INSL3 can also act as a motility-enhancing factor on PC-3 human prostate carcinoma cells.[35] MMPs and their tissue inhibitors of metalloproteinases (TIMPs) have been identified to potentially facilitate relaxin's effects on cellular migration and ECM invasion.[31,36–38] In human mammary carcinoma cells, relaxin was shown to affect the expression profile of specific MMPs[32] and one report indicated a correlation between increased relaxin serum levels and metastases in human breast cancer patients.[39] We demonstrated a strong correlation between relaxin-mediated induction of specific MMPs and degradation of extracellular matrix (ECM) components resulting in enhanced migration of canine mammary carcinoma cells.[15] In the present study, we have identified the highly potent proteolytic lysosomal acid hydrolases of the cathepsin family as novel relaxin target enzymes in thyroid carcinoma cells and demonstrated a significantly increased elastinolytic activity of the FTC-133-RLN2 clones. Cathepsin proteases have been implicated in numerous pathologies, including inflammatory processes,[40] Alzheimer's disease,[41,42] and metastasis of tumor cells.[43–46] Both cathepsins, cath-D and cath-L, produced by all transfectants studied are reported to be active in human thyroid carcinoma tissues.[46–48] The significant up-regulation in the production and secretion of cath-L forms in RLN2 transfectants correlated with an enhanced elastinolytic activity and the ability to invade elastin matrices. Known as a powerful protease promoting migration and basement membrane degradation by tumor cells,[49–51] cath-L also confers to endothelial progenitor cells the proteolytic, promigratory capacity essential for neovascularization *in vivo*.[52] Most apparent for procath-L, relaxin affected the cytosolic distribution of cath-L in RLN2 transfectants. The polar to perinuclear distribution of (pro)cath-L in these RLN2 clones as opposed to an even granular cytoplasmic distribution in the EGFP controls seem to reflect a specific relaxin-induced state of differentiation because our data clearly identified relaxin as a differentiation factor and not a mitogen for human thyroid carcinoma cells. Expression and subcellular distribution of cath-L was shown to be affected by the state of enterocytic differentiation of the human colon carcinoma cell line HT-29.[53] Although the exact role for relaxin in this process is unclear, it may involve changes in the endosome to lysosome routing of mannose-6-phosphate-tagged cath-L because mannose-6-phosphate receptors[54] displayed a cytoplasmic distribution similar to that detected for procath-L in the RLN2 transfectants. Interestingly, no change in the cytoplasmic distribution for cath-D was observed in the RLN2 transfectants suggesting a specific role for relaxin in cath-L containing vesicular trafficking.

In thyroid carcinoma tissues, cath-D concentrations are significantly higher and correlate with tumor size and stage.[48] Relaxin transfectants had significantly increased levels of procath-D and, like in human breast cancer, procath-D was the major secreted glycoprotein in all RLN2 transfectants investigated. In contrast to human breast cancer, estrogens are not regarded as regulators of cath-D production in thyroid carcinoma tissues.[47,48] Our finding of abundant production of relaxin in thyroid neoplasia implicates relaxin as a potential novel local regulator of procath-D production in human thyroid carcinoma. By up-regulating the production and secretion of (pro)cath-D and -L, relaxin may not only enhance the local proteolytic activity and tumor cell invasiveness but will also promote tumor angiogenic capacity and survival of human thyroid carcinoma cells.[55–58]

In summary, RLN2 and its receptor LGR7 are expressed in the majority of human thyroid carcinoma tissues and exert, in an autocrine/paracrine manner, enhanced tumor-promoting activity and invasiveness in neoplastic thyrocytes. These findings provide the rationale for future oncostatic strategies aimed at suppressing relaxin-mediated signal transduction pathways as a novel therapeutic approach in human thyroid cancer.

Acknowledgments

We thank Ms. Christine Froehlich, Maria Riedel, Katrin Hammje, Rita Medek, and Elisabeth Schlueter for their excellent technical assistance; Dr. Laura Parry, Department of Zoology, University of Melbourne, Melbourne, Australia, for generously providing human RLN2; Dr. Bernhard Steinetz, Nelson Institute of Environmental Medicine, New York University Medical Center, Tuxedo, NY, for his kind gift of polyclonal R6 antiserum against relaxin; and Drs. S.Y. Hsu and A.J.W. Hsueh, Stanford University School of Medicine, Stanford, CA, for generously donating the polyclonal antiserum against human LGR7.

References

1. Ivell R, Einspanier A: Relaxin peptides are new global players. Trends Endocrinol Metab 2002, 13:343–348
2. Silvertown JD, Summerlee AJ, Klonisch T: Relaxin-like peptides in cancer. Int J Cancer 2003, 107:513–519
3. Plunkett ER, Squires BP, Richardson SJ: The effect of relaxin on thyroid weights in laboratory animals. J Endocrinol 1960, 21:241–246
4. Plunkett ER, Squires BP, Heagy FC: Effect of relaxin on thyroid function in the rat. J Endocrinol 1963, 26:331–338
5. Braverman LE, Ingbar SH: Effects of preparations containing relaxin on thyroid function in the female rat. Endocrinology 1963, 72:337–341
6. Adham IM, Burkhardt E, Benahmed M, Engel W: Cloning of a cDNA for a novel insulin-like peptide of the testicular Leydig cells. J Biol Chem 1993, 268:26668–26672
7. Pusch W, Balvers M, Ivell R: Molecular cloning and expression of the relaxin-like factor in the mouse testis. Endocrinology 1996, 137:3009–3013
8. Hsu SY, Nakabayashi K, Nishi S, Kumagai J, Kudo M, Sherwood OD, Hsueh AJW: Activation of orphan receptors by the hormone relaxin. Science 2002, 295:671–674
9. Bartsch O, Bartlick B, Ivell R: Phosphodiesterase 4 inhibition synergized with relaxin signaling to promote decidualization of human endometrial stromal cells. J Clin Endocrinol Metab 2004, 89:324–334
10. Bartsch O, Bartlick B, Ivell R: Relaxin signalling links tyrosine phosphorylation to phosphodiesterase and adenylyl cyclase activity. Mol Hum Reprod 2001, 7:799–809
11. Parsell DA, Mak JY, Amento EP, Unemori EN: Relaxin binds to and elicits a response from cells of the human monocytic cell line, THP-1. J Biol Chem 1996, 271:27936–27941
12. Bogatcheva NV, Truong A, Feng S, Engel W, Adham IM, Agoulnik AI: GREAT/LGR8 is the only receptor for insulin-like 3 peptide. Mol Endocrinol 2003, 17:2639–2646
13. Hombach-Klonisch S, Hoang-Vu C, Kehlen A, Hinze R, Holzhausen HJ, Weber E, Fischer B, Dralle H, Klonisch T: INSL-3 is expressed in human hyperplastic and neoplastic thyrocytes. Int J Oncol 2003, 22:993–1001
14. Tashima LS, Mazoujian G, Bryant-Greenwood GD: Human relaxins in normal, benign and neoplastic breast tissue. J Mol Endocrinol 1994, 12:351–364
15. Silvertown JD, Geddes BJ, Summerlee AJS: Adenovirus-mediated expression of human prorelaxin promotes the invasive potential of canine mammary cancer cells. Endocrinology 2003, 144:3683–3691
16. Radestock Y, Hoang-Vu C, Hombach-Klonisch S: Relaxin downregulates the calcium binding protein S100A4 in MDA-MB-231 human breast cancer cells. Ann NY Acad Sci 2005, 1041:462–469
17. Klonisch T, Mustafa T, Bialek J, Radestock Y, Holzhausen H-J, Dralle H, Hoang-Vu C, Hombach-Klonisch S: Human medullary thyroid carcinoma (MTC): a source and potential target for relaxin-like hormones. Ann NY Acad Sci 2005, 1041:449–461
18. Bigazzi M, Brandi ML, Bani G, Sacchi TB: Relaxin influences the growth of MCF-7 breast cancer cells. Mitogenic and antimitogenic action depends on peptide concentration. Cancer 1992, 70:639–643
19. Binder C, Hagemann T, Hausen B, Schulz M, Einspanier A: Relaxin enhances in-vitro invasiveness of breast cancer cell lines by up-regulation of matrix metalloproteinases. Mol Hum Reprod 2002, 8:789–796
20. Sambrook J, Fritsch EF, Maniatis T: Molecular Cloning—A Laboratory Manual, vol. 3, ed 2. Edited by Maniatis T. Cold Spring Harbor, Cold Spring Harbor Laboratory Press, 1989, appendix E5
21. Dschietzig T, Richter C, Bartsch C, Laule M, Armbruster FP, Baumann G, Stangl K: The pregnancy hormone relaxin is a player in human heart failure. FASEB J 2001, 15:2187–2195
22. Fiebiger E, Meraner P, Weber E, Fang IF, Stingl G, Ploegh H, Maurer D: Cytokines regulate proteolysis in major histocompatibility complex class II-dependent antigen presentation by dendritic cells. J Exp Med 2001, 193:881–892
23. Tolosa E, Li W, Yasuda Y, Wienhold W, Denzin LK, Lautwein A, Driessen C, Schnorrer P, Weber E, Stevanovic S, Kurek R, Melms A, Bromme D: Cathepsin V is involved in the degradation of invariant chain in human thymus and is overexpressed in myasthenia gravis. J Clin Invest, 2003, 112:517–526
24. Yasuda Y, Li Z, Greenbaum D, Bogyo M, Weber E, Bromme D: Cathepsin V, a novel and potent elastolytic activity expressed in activated macrophages. J Biol Chem 2004, 279:36761–36770
25. Chapman HA, Riese RJ, Shi GP: Emerging roles for cysteine proteases in human biology. Annu Rev Physiol 1997, 59:63–88
26. Kamat AA, Feng S, Bogatcheva NV, Truong A, Bishop CE, Agoulnik AI: Genetic targeting of relaxin and insulin-like factor 3 receptors in mice. Endocrinology 2004, 145:4712–4720
27. Zarreh-Hoshyari-Khah R, Bartsch O, Einspanier A, Pohnke Y, Ivell R: Bioactivity of recombinant prorelaxin from the marmoset monkey. Regul Pept 2001, 97:139–146
28. Marriott D, Gillece-Castro B, Gorman CM: Prohormone convertase-1 will process prorelaxin, a member of the insulin family of hormones. Mol Endocrinol 1992, 6:1441–1450
29. Vu AL, Green CB, Roby KF, Soares MJ, Fei DT, Chen AB, Kwok SC: Recombinant porcine prorelaxin produced in Chinese hamster ovary cells is biologically active. Life Sci 1993, 52:1055–1061
30. Masini E, Bani D, Bello MG, Bigazzi M, Mannaioni PF, Sacchi TB: Relaxin counteracts myocardial damage induced by ischemia-reperfusion in isolated guinea pig hearts: evidence for an involvement of nitric oxide. Endocrinology 1997, 138:4713–4720
31. Kamat AA, Feng S, Agoulnik IU, Kheradmand F, Bogatcheva NV, Coffey D, Sood AK, Agoulnik AI: The role of relaxin in endometrial cancer. Cancer Biol Ther 2005, 5:e1–e7
32. Binder C, Hagemann T, Husen B, Schulz M, Einspanier A: Relaxin enhances in-vitro invasiveness of breast cancer cell lines by up-regulation of matrix-metalloproteinases. Mol Hum Reprod 2002, 8:789–796
33. Wyatt TA, Sisson JH, Forget MA, Bennett RG, Hamel FG, Spurzem JR: Relaxin stimulates bronchial epithelial cell PKA activation, migration, and ciliary beating. Exp Biol Med 2002, 227:1047–1053
34. Unemori EN, Lewis M, Constant J, Arnold G, Grove BH, Normand J, Deshpande U, Salles A, Pickford LB, Erikson ME, Hunt TK, Huang X: Relaxin induces vascular endothelial growth factor expression and angiogenesis selectively at wound sites. Wound Repair Regen 2000, 8:361–370
35. Klonisch T, Müller-Huesmann H, Riedel M, Kehlen A, Bialek J, Radestock Y, Holzhausen H-J, Steger K, Ludwig M, Weidner W, Hoang-Vu C, Hombach-Klonisch S: INSL3 in the benign hyperplastic and neoplastic human prostate gland. Int J Oncol 2005, 27:307–315
36. Khasigov PZ, Podobed OV, Gracheva TS, Salbiev KD, Grachev SV, Berezov TT: Role of matrix metalloproteinases and their inhibitors in tumor invasion and metastasis. Biochemistry 2003, 68:711–717
37. Jiang Y, Goldberg ID, Shi YE: Complex roles of tissue inhibitors of metalloproteinases in cancer. Oncogene 2002, 21:2245–2252
38. Kraiem Z, Korem S: Matrix metalloproteinases and the thyroid. Thyroid 2000, 10:1061–1069
39. Binder C, Simon A, Binder L, Hagemann T, Schulz M, Emons G, Trumper L, Einspanier A: Elevated concentrations of serum relaxin are associated with metastatic disease in breast cancer patients. Breast Cancer Res Treat 2004, 87:157–166
40. Lennon-Dumenil AM, Bakker AH, Wolf-Bryant P, Ploegh HL, Lagaudriere-Gesbert C: A closer look at proteolysis and MHC-class-II-restricted antigen presentation. Curr Opin Immunol 2002, 14:15–21
41. Lauritzen E, Moller S, Leerhoy J: Leucocyte migration inhibition in vitro with inhibitors of aspartic and sulphhydryl proteinases. Acta Pathol Microbiol Immunol Scand [C] 1984, 92:107–112
42. Cataldo AM, Nixon RA: Enzymatically active lysosomal proteases are associated with amyloid deposits in Alzheimer brain. Proc Natl Acad Sci USA 1990, 87:3861–3865
43. Adamec E, Mohan PS, Cataldo AM, Vonsattel JP, Nixon RA: Up-regulation of the lysosomal system in experimental models of neuronal injury: implications for Alzheimer's disease. Neuroscience 2000, 100:663–675
44. Leto G, Tumminello FM, Crescimanno M, Flandina C, Gebbia N: Cathepsin D expression levels in nongynecological solid tumors: clinical and therapeutic implications. Clin Exp Metastasis 2004, 21:91–106
45. Leto G, Gebbia N, Rausa L, Tumminello FM: Cathepsin D in the malignant progression of neoplastic diseases (review). Anticancer Res 1992, 12:235–240
46. Metaye T, Kraimps JL, Goujon JM, Fernandez B, Quellard N, Ingrand P, Barbier J, Begon F: Expression, localisation, and thyrotropin regulation of cathepsin D in human thyroid tissues. J Clin Endocrinol Metab 1997, 82:3383–3388

47. Metaye T, Millet C, Kraimps JL, Aubouin B, Barbier J, Begon F: Estrogen receptors and cathepsin D in human thyroid tissue. Cancer 1993, 72:1991–1996
48. Kraimps JL, Metaye T, Millet C, Margerit D, Ingrand P, Goujon JM, Levillain P, Babin P, Begon F, Barbier J: Cathepsin D in normal and neoplastic thyroid tissues. Surgery 1995, 118:1036–1040
49. Krueger S, Kellner U, Buehling F, Roessner A: Cathepsin L antisense oligonucleotides in a human osteosarcoma cell line: effects on the invasive phenotype. Cancer Gene Ther 2001, 8:522–528
50. Kirschke H, Eerola R, Hopsu-Havu VK, Bromme D, Vuorio E: Antisense RNA inhibition of cathepsin L expression reduces tumorigenicity of malignant cells. Eur J Cancer 2000, 36:787–795
51. Dohchin A, Suzuki JI, Seki H, Masutani M, Shiroto H, Kawakami Y: Immunostained cathepsins B and L correlate with depth of invasion and different metastatic pathways in early stage gastric carcinoma. Cancer 2000, 89:482–487
52. Urbich C, Heeschen C, Aicher A, Sasaki K, Bruhl T, Farhadi MR, Vajkoczy P, Hofmann WK, Peters C, Pennacchio LA, Abolmaali ND, Chavakis E, Reinheckel T, Zeiher AM, Dimmeler S: Cathepsin L is required for endothelial progenitor cell-induced neovascularization. Nat Med 2005, 11:206–213
53. De Stefanis D, Demoz M, Dragonetti A, Houri JJ, Ogier-Denis E, Codogno P, Baccino FM, Isidoro C: Differentiation-induced changes in the content, secretion, and subcellular distribution of lysosomal cathepsins in the human colon cancer HT-29 cell line. Cell Tissue Res 1997, 289:109–117
54. Von Figura K, Hasilik A: Lysosomal enzymes and their receptors. Annu Rev Biochem 1986, 55:167–193
55. Laurant-Matha V, Maruani-Herrmann S, Prebois C, Beaujouin M, Glondu M, Noel A, Alvarez-Gonzalez ML, Blacher S, Coopman P, Baghdiguian S, Gilles C, Loncarek J, Freiss G, Vignon F, Liaudet-Coopman E: Catalytically inactive human cathepsin D triggers fibroblast invasive growth. J Cell Biol 2005, 168:489–499
56. Koike M, Shibata M, Ohsawa Y, Nakanishi H, Koga T, Kametaka S, Waguri S, Momoi T, Kominami E, Peters C, Von Figura K, Saftig P, Uchiyama Y: Involvement of two different cell death pathways in retinal atrophy of cathepsin D-deficient mice. Mol Cell Neurosci 2003, 22:146–161
57. Nakanishi H, Zhang J, Koike M, Nsihioku T, Okamoto Y, Kominami E, Von Figura K, Peters C, Yamamoto K, Saftig P, Uchiyama Y: Involvement of nitric oxide released from microglia-macrophages in pathological changes of cathepsin D-deficient mice. J Neurosci 2001, 21:7526–7533
58. Saftig P, Hetman M, Schmahl W, Weber K, Heine L, Mossmann H, Koster A, Hess B, Evers M, Von Figura K, Peters C: Mice deficient for the lysosomal proteinase cathepsin D exhibit progressive atrophy of the intestinal mucosa and profound destruction of lymphoid cells. EMBO J 1995, 14:3599–3608
59. Radestock Y, Hoang-Vu C, Hombach-Klonisch S: Relaxin downregulates the calcium binding protein S100A4 in MDA-MB-231 human breast cancer cells. Ann NY Acad Sci 2005, 1041:462–469